CHAPTER VI

RESIDENCE TIME ESTIMATION METHOD

6.1. Description of the compressible flow model as a tool to estimate the residence time

6.1.1. Thermodynamic model

A thermodynamic model was used to evaluate the changes in the compressibility factor of the reaction mixture, and was established as being suitable as long as the reaction proceeds in the tubular reactor [85, 89]. However, experimental fluid properties and / or experimental vapor-liquid equilibrium (VLE) data of binary sub-systems are required to find the most suitable thermodynamic model in order to predict such properties and fluid physical state for the reaction system. In actuality, the real reaction system composed of various types of triglyceride, e.g., tripalmitin, triolein, palmito-diolein and palmito-linoleo-olein etc., five to eight types of fatty acid methyl esters (FAMEs), and reaction intermediates, such as mono- and diglycerides. To simplify the calculation, we assumed that the reaction system consists of methanol, triolein, methyl oleate and glycerol, with triolein and methyl oleate representing the palm olein oil and biodiesel (mixture of FAMEs), respectively, in accordance with the major fatty acid composition of palm olein oil as mentioned in Section 3.3.2. Therefore, we employed the existing VLE measurements of triolein + methanol, methyl oleate + methanol and glycerol + methanol binary systems from the literature. This simplification was chosen because of the availability of experimental data in the literature for these binary systems, but not more complex ones.

It is important to note here that the high pressure / high temperature VLE or density experimental data for the triolein / methanol mixture are quite difficult to obtain because of the high reactivity of the mixture under these high operating pressures and temperatures. To find the best model to predict the thermodynamic behavior of the quaternary mixture, we intended to test the classical Peng-Robinson equation of state (PR) [90] with the mixing rules developed by Huron and Vidal [91] and modified by Michelsen [92] (MHV2 mixing rules). This approach allows the cubic equation of state PR, suitable for high pressure but poor for mixtures containing polar compounds, to be applied for high-pressure calculations of mixtures involving polar compounds. As the

MHV2 mixing rules are based on the calculation of the excess Gibbs energy at zero pressure, this also requires a suitable activity coefficient model, in addition to the equation of state. Here we decided to use the UNIQUAC [93] activity coefficient model, because the coupling of this model to a cubic EOS via the MHV2 mixing rules has already been shown to be a good model for predicting the high-pressure fluid phase equilibria of mixtures containing polar compounds [94], as it is the case here. Moreover, this model is available in Simulis® Thermodynamics (ProSim, France), commercial software for the calculation of fluid phase equilibria and fluid properties.

6.1.2. Compressible flow model

The general mole balance in a tubular reactor [95] and the transesterification kinetics of refined-bleached-de-odorized (RBD) palm oil in SCM [72] are illustrated in equations (6.1) and (6.2) respectively

$$\frac{dX_A}{dV} = \frac{-r_A}{F_{A0}} \tag{6.1}$$

$$-r_A = kC_A^{0.95}C_B^{1.05} \tag{6.2}$$

where X, V, r_A and F_{A0} are conversion, reactor volume (m^3), rate of transesterification reaction ($mol/s.m^3$) and molar flow rate at reactor inlet (mol/s), respectively. The subscript A and B referred to triolein and methanol, respectively.

The chemical kinetics of RBD palm oil was investigated in a 4.7-mL batch reactor at 30.0 MPa within the temperature range of 200 to 400 °C, a methanol to oil molar ratio range of 3:1 to 80:1, and a reaction time range of 0.5 to 30 min The rate constant and reaction order were found by an integral method or numerical fitting of the experimental data to the kinetic model, resulting in a high coefficient of determination (R^2) value, at 0.9578, even though it does not include the thermal degradation reaction [72]. The rate constant was defined as a function of temperature as shown in equation (6.3).

$$k = 4.34\times10^5 \times \exp\left(-\frac{1.05\times10^5}{RT}\right) \tag{6.3}$$

where k, R and T are the rate constant (m^3/mol.s), universal gas constant (J/mol.K) and temperature (K), respectively

In a continuous isothermal reactor, concentration and total molar flow rate of mixture corresponding to inlet flow rate can be written as Equation (6.4) and (6.5) respectively.

$$C = \frac{F}{v_m} \tag{6.4}$$

$$v_m = v_{m0}\left(\frac{z_m}{z_{m0}}\right)\frac{P_0}{P} \tag{6.5}$$

where C, F, v, z, and P are concentration (mol/m^3), molar flow rate (mol/s), volumetric flow rate (m^3/s), compressibility factor and pressure (MPa), respectively. The subscripts m and 0 refer to mixture and reactor inlet, respectively.

From the experimental observations, values of pressure were found to be slightly different between the high-pressure pump and the reactor outlet. Therefore, the zero pressure drop assumption was applied and P kept equal to P_0. Finally, all equations were combined and rearranged to model the conversion change along the tubular reactor, as shown in equation (6.6).

From the experimental observation, values of pressure were found to be slightly different between the high-pressure pump and the reactor outlet; therefore, the zero pressure drop assumption was applied and P kept equal to P_0. Finally, all Equations were combined and rearranged to model the conversion change along the tubular reactor as shown in Equation (6.6).

$$\frac{dX_A}{dL} = \frac{kAF_{A0}}{v_{m0}^2}\left(1-X_A\right)^{0.95}\left(\frac{F_{B0}}{F_{A0}} - 3X_A\right)^{1.05}\left(\frac{z_{m0}}{z_m}\right)^2 \tag{6.6}$$

This governing Equation was numerically solved for conversion prediction as function of reactor length employing the Runge-Kutta method using the Matlab® software (ODE45) coupled with the Simulis® Thermodynamic toolbox, to evaluate the compressibility factor and the physical state of the mixture as the reaction proceeds inside the tube. Note that the Matlab® software read the compressibility factor as function of conversion through Simulis® Thermodynamic toolbox. The compressibility factor of the quaternary mixture was estimated by the thermodynamic model described in Section 5.1.1 with adjusted binary interaction parameters.

Finally, the calculated mole fraction of methyl oleate which represents ME content in biodiesel product was estimated from final conversion and compared with experimental results. It should be notice that the simple compressible flow model is a tool

to estimate the molar volume of the mixture and then use for calculating the residence time of biodiesel production with SCM

Additionally, assuming a constant compressibility factor leads to equation (6) being reduced to equation (6.7). The computation was done to estimate the magnitude of the effect of compressibility factor development upon ME content and solved by the Runge-Kutta 4th order method using the Matlab® software. The volumetric flow rate of the mixture at the inlet of the reactor (v_{m0}) was determined by the PR-MHV2-UNIQUAC thermodynamic model.

$$\frac{dX_A}{dL} = \frac{kAF_{A0}}{v_{m0}^2}\left(1-X_A\right)^{0.95}\left(\frac{F_{B0}}{F_{A0}}-3X_A\right)^{1.05} \tag{6.7}$$

6.2. Fitting of the thermodynamic model and binary interaction parameters

The VLE studies of binary systems from the literature [14, 17, 55] were fitted by the PR-MHV2-UNIQUAC thermodynamic model, in order to obtain a set of binary interaction parameters for UNIQUAC as a function of temperature. This fitting was carried out using the least square method with a Simulis® Thermodynamics add-in, inserted in MS-Excel worksheet. The critical properties of triolein, methyl oleate and glycerol were estimated by the Constantinou–Gani group-contribution method [74, 75]. The interaction coefficients are given in Table 6.1.

Table 6.1 Calculated binary interaction coefficients for UNIQUAC model.

Binary mixture	Ref.	Type of data	A_{12} (K)	A_{21} (K)
Triolein + methanol	[14]	Isothermal VLE 473 to 503K	$11559.00 - 23.43T$	$-8072.30 + 16.85T$
Methyl oleate + methanol	[55]	Isothermal VLE 523 to 573 K	$1698.00 - 3.60T$	$-5713.30 + 12.06T$
Glycerol + methanol	[17]	Isothermal VLE 493 to 573 K	$1850.00 - 4.02T$	$-4801.17 + 10.48T$

The VLE experimental data for triolein + methanol, methyl oleate + methanol and glycerol + methanol, and the results from PR-MHV2-UNIQUAC model are shown in Tables 6.2 to 4 and Figures 6.2 to 6.4. The relative error of methanol mole fraction in liquid (x) and vapor (y) phase was calculated from equation (6.8). Thus, the minus and plus sign illustrated the under and overestimated value respectively.

$$\%Relative\ Error = \frac{(Calculated\ value - Experimental\ value)}{Experimental\ value} \times 100 \quad (6.8)$$

The PR-MHV2-UNIQUAC model had maximum relative error of 5% for the triolein + methanol and 3% for methyl oleate + methanol, whereas it had maximum relative error of 10% for the glycerol + methanol system that was higher than the relative error of the specific models in the literature due to the difference polarity of those mixtures, especially for triolein + methanol and glycerol + methanol. The polarity of the compounds can be ranked by their dielectric constants, being 41.14, 32.60, 3.12 and 3.11 for glycerol, methanol, methyl oleate and triolein, respectively [96]. Thus, the attractive and repulsive forces within the glycerol + methanol system were somewhat higher than both the triolein + methanol and methyl oleate + methanol systems, and affected the thermodynamic model for VLE prediction. For example, the Peng–Robinson (PR EOS) and the van der Waals (VdW) mixing rule models were tested on the triolein + methanol system and give an approximately 2% relative error [19], whereas the Peng–Robinson Stryjek–Vera (PR-SV) EOS and ASOG mixing rule (PRASOG model) give an approximately 3% relative error for the glycerol + methanol VLE system [17].

Table 6.2 Methanol mole fraction in liquid (x) and vapor (y) phase of triolein + methanol VLE [14].

T	P	Experimental result		Calculated result		%Relative	%Relative
(K)	(Bar)	x	y	x	y	Error of x	Error of y
473	39.7	0.9744	0.9997	0.9800	1.0000	0.575	0.030
473	36.7	0.9413	0.9998	0.9543	1.0000	1.383	0.020
473	34.1	0.9087	0.9996	0.9269	1.0000	2.004	0.040
473	29.2	0.8540	0.9996	0.8750	1.0000	2.461	0.040
483	45.3	0.9655	0.9999	0.9800	1.0000	1.502	0.010
483	42.5	0.9557	0.9999	0.9665	1.0000	1.125	0.009
483	39.9	0.9292	1.0000	0.9337	1.0000	0.487	0.000
483	31.1	0.8642	0.9998	0.8166	1.0000	-5.504	0.020
493	48.6	0.9755	0.9997	0.9773	1.0000	0.187	0.029
493	48.0	0.9729	0.9997	0.9756	1.0000	0.276	0.028
493	43.5	0.9569	0.9999	0.9566	1.0000	-0.027	0.008
493	40.4	0.9170	0.9999	0.9287	1.0000	1.271	0.009

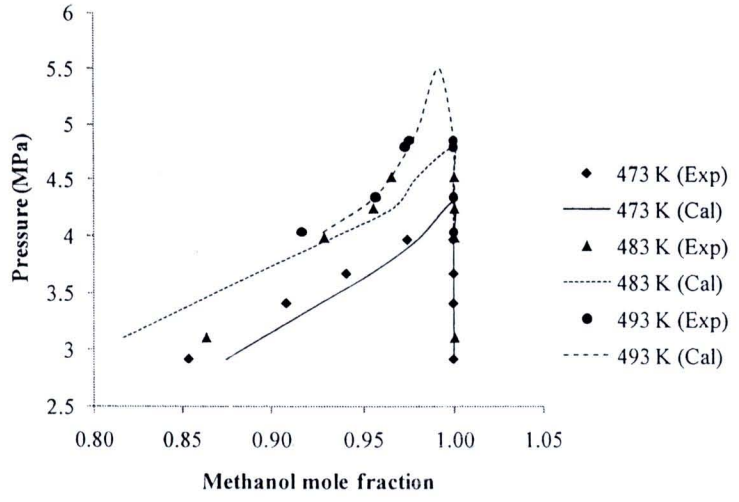

Figure 6.1 Experimental (Exp) and calculated (Cal) P-x-y diagram of triolein + methanol VLE. The experimental data were measured twice at each point and they have the average deviations of 3.09 % and 0.15 % for liquid and vapor phase measurement, respectively [14].

Table 6.3 The methanol mole fraction in liquid (x) and vapor (y) phase of methyl oleate + methanol VLE [55].

T	P	Experimental result		Calculated result		%Relative	%Relative
(K)	(Bar)	x	y	x	y	Error of x	Error of y
523	24.5	0.4650	1.0000	0.4521	0.9951	-2.780	-0.489
523	53.5	0.7310	0.9999	0.7326	0.9958	0.219	-0.316
523	64.6	0.8140	1.0000	0.8106	0.9954	-0.415	-0.463
523	70.2	0.8630	1.0000	0.8465	0.9949	-1.906	-0.510
523	78.0	0.9160	1.0000	0.8949	0.9937	-2.300	-0.633
548	45.9	0.5750	1.0000	0.5716	0.9930	-0.597	-0.697
548	61.0	0.6930	1.0000	0.6750	0.9936	-2.593	-0.643
548	79.0	0.7900	1.0000	0.7724	0.9935	-2.233	-0.647
548	88.0	0.8380	0.9930	0.8125	0.9933	-3.043	0.029
548	94.8	0.8610	0.9910	0.8394	0.9930	-2.508	0.205
573	60.3	0.6070	1.0000	0.6204	0.9889	2.209	-1.106
573	70.1	0.6990	1.0000	0.6764	0.9901	-3.238	-0.993
573	83.9	0.7510	0.9960	0.7440	0.9916	-0.936	-0.440
573	102.5	0.8330	0.9880	0.8172	0.9942	-1.896	0.623
573	114.5	0.8600	0.9860	0.8532	0.9959	-0.795	1.001

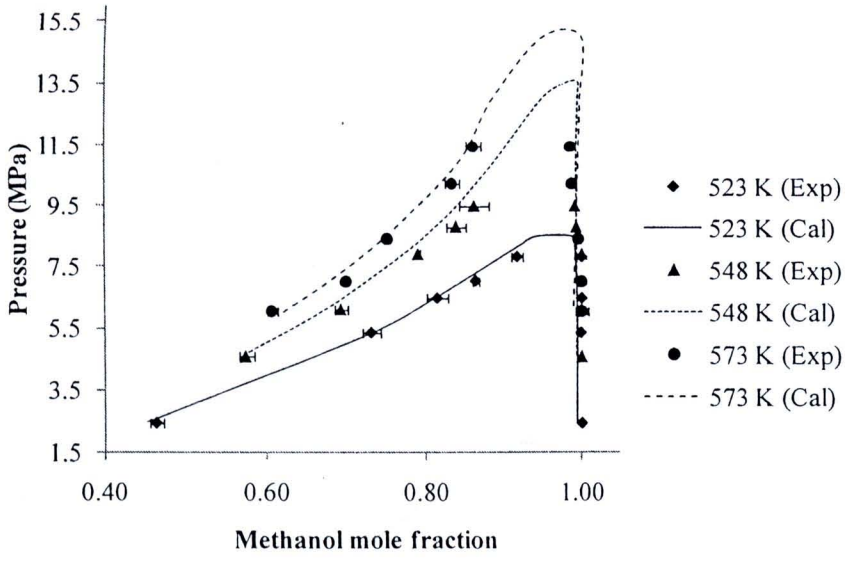

Figure 6.2 Experimental (Exp) and calculated (Cal) P-x-y diagram of methyl oleate + methanol VLE. The experimental data were measured four times at each point and the average deviations were shown in figure as error bars [55].

Table 6.4 The methanol mole fraction in liquid (x) and vapor (y) phase of glycerol + methanol VLE [17].

T	P	Experimental result		Calculated result		%Relative	%Relative
(K)	(Bar)	x	y	x	y	Error of x	Error of y
493	30.3	0.4780	1.0000	0.4898	0.9924	2.464	-0.757
493	34.1	0.5500	1.0000	0.5577	0.9927	1.392	-0.729
493	38.6	0.6450	1.0000	0.6503	0.9930	0.825	-0.703
493	42.3	0.7010	1.0000	0.7418	0.9932	5.821	-0.676
493	46.7	0.8500	1.0000	0.8523	0.9939	0.276	-0.607
493	51.2	0.9650	1.0000	0.9299	0.9955	-3.642	-0.452
523	46.4	0.4840	1.0000	0.4681	0.9816	-3.287	-1.836
523	52.1	0.5650	1.0000	0.5248	0.9812	-7.119	-1.882
523	60.8	0.6890	1.0000	0.6217	0.9795	-9.766	-2.051
523	67.9	0.8070	1.0000	0.7269	0.9769	-9.925	-2 312
523	71.6	0.8680	1.0000	0.8055	0.9749	-7.197	-2.510
543	54.1	0.4310	1.0000	0.4506	0.9708	4.546	-2.921
543	61.8	0.5090	1.0000	0.5084	0.9698	-0.117	-3.024
543	69.9	0.5920	1.0000	0.5709	0.9674	-3.562	-3.259
543	79.1	0.6970	1.0000	0.6479	0.9623	-7.043	-3.770
543	86.1	0.7800	0.9900	0.7175	0.9546	-8.008	-3.576

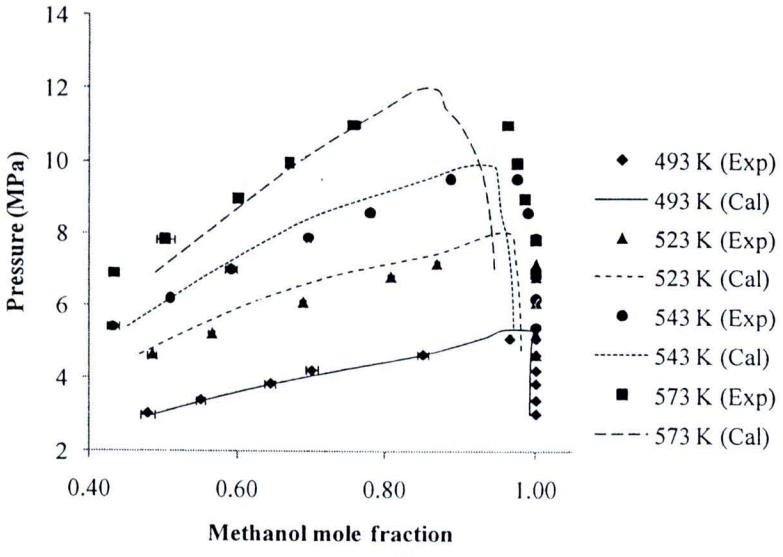

Figure 6.3 Experimental (Exp) and calculated (Cal) P-x-y diagram of glycerol + methanol VLE. The experimental data were measured four to six times at each point and the average deviations were shown in figure as error bars [17].

6.3. ME content prediction by the compressible flow model

The compressible flow model was tested in various reacting conditions as shown in Table 6.5, and then in Figure 6.5, observed values were plotted against calculated values. Furthermore, the %relative error and residence time for each condition in Table 6.5 can be calculated by Equation (6.8) and (6.9), respectively. The residence time estimation procedure is described in Section 6.4.

$$\tau = \int_V \frac{dV}{u} \tag{6.9}$$

Table 6.5 The observed and calculated ME content from various reacting conditions.

No.	T (°C)	P (MPa)	MeOH:Oil molar ratio	τ (min)	ME content (%)			%Relative error	
					Exp. value	Cal. value*	Cal. value **	Cal. value*	Cal. value **
1	278	35	12.0	42.21	35.75	35.18	41.70	-1.6	16.6
2	280	20	14.4	42.36	37.25	35.81	41.95	-3.9	12.6
3	280	35	41.4	46.52	27.09	29.17	31.13	7.7	14.9
4	282	20	38.9	45.25	31.95	30.82	33.16	-3.5	3.8
5	285	35	21.0	44.65	42.01	39.65	45.32	-5.6	7.9
6	300	20	27.8	39.71	68.50	68.60	81.03	0.2	18.3
7	300	35	36.7	40.55	65.67	69.53	81.56	5.9	24.2
8	300	35	39.6	40.57	69.82	78.42	87.05	12.3	24.7
9	320	20	23.7	34.04	80.55	83.88	97.19	4.1	20.7
10	320	20	23.7	34.05	76.38	82.71	94.20	8.3	23.3
11	320	35	37.3	41.96	57.68	69.40	80.86	20.3	40.2
12	320	35	22.8	40.08	65.78	79.20	90.10	20.4	36.9
13	320	35	38.7	41.00	72.42	76.59	86.60	5.8	19.6
14	350	20	24.8	35.84	73.15	88.63	98.41	21.2	34.5
15	350	20	16.9	36.17	74.24	87.76	97.87	18.2	31.8
16	350	20	27.8	37.48	63.26	84.70	95.69	33.9	51.3
17	350	35	17.1	35.67	69.35	89.95	99.14	29.7	42.9
18	350	35	35.2	35.62	69.94	90.07	99.18	28.8	41.8
19	350	35	27.8	38.53	66.41	86.86	96.72	30.8	45.6
20	350	35	35.9	35.41	69.19	90.05	99.22	30.2	43.4
21	352	20	17.1	34.05	77.30	90.42	99.54	17.0	28.8
22	352	35	43.4	38.39	78.00	87.39	97.01	12.0	24.4

*As calculated by * equation (6.6) or ** equation (6.7) (see the text)*

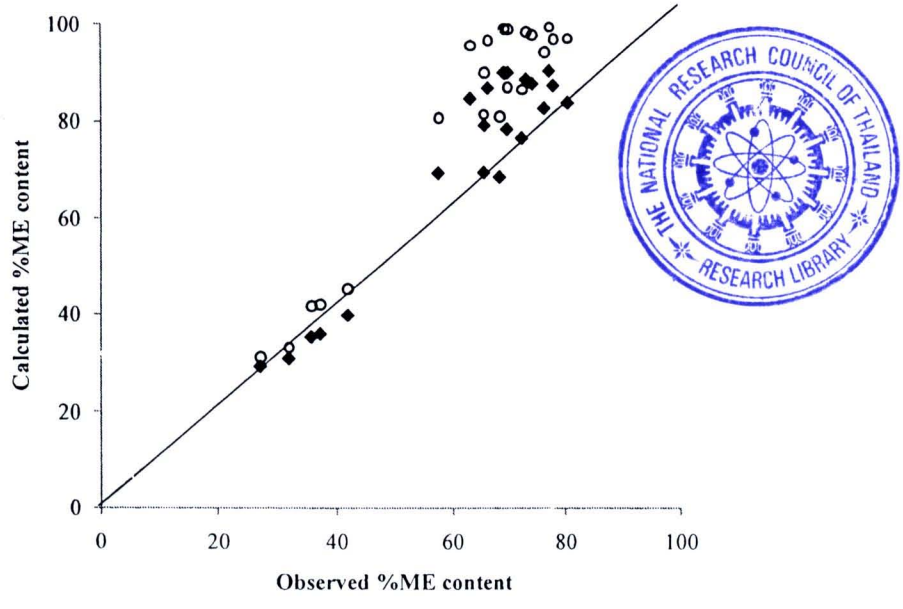

Figure 6.5 The plot of experimented and calculated ME content by Eq. 6.6 (◆) or Eq.6.7 (○).

According to Figure 6.5, the model was good for estimating %ME content at temperature range of 280 – 320 °C, while calculated %methyl esters at 320 – 350 °C were overestimated. It was noticed that %relative error of calculated values from Equation (6.6) was increasing with reaction temperature as illustrated in Figure 6.6, whereas the pattern of %relative error with methanol to oil molar ratio and pressure were scattered as shown in Figure 6.7 and 6.8 respectively.

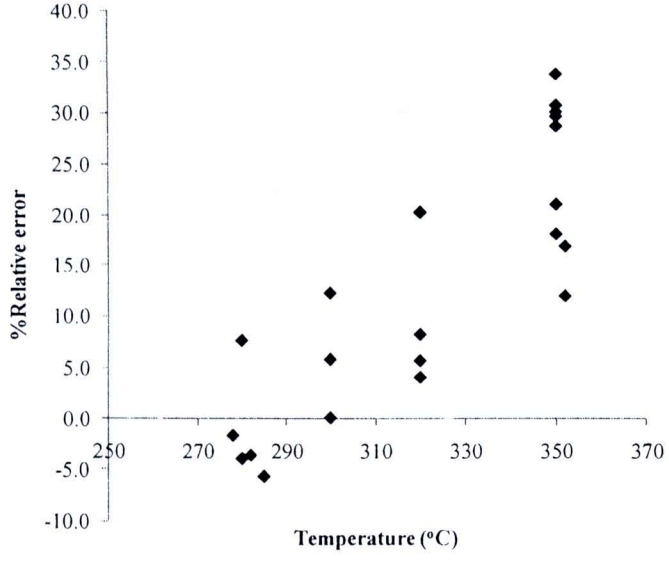

Figure 6.6 The relationship between percentage of relative error of calculated value from Eq. 6.6 and reaction temperature.

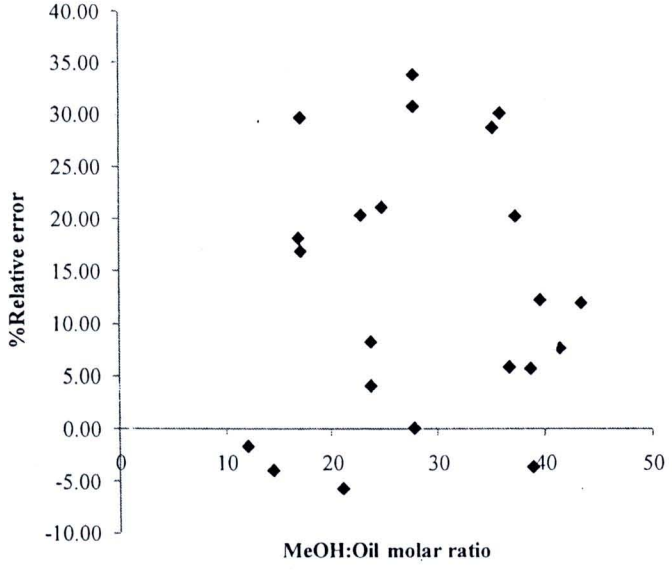

Figure 6.7 The relationship between percentage of relative error of calculated value from Eq. 6.6 and methanol to oil molar ratio.

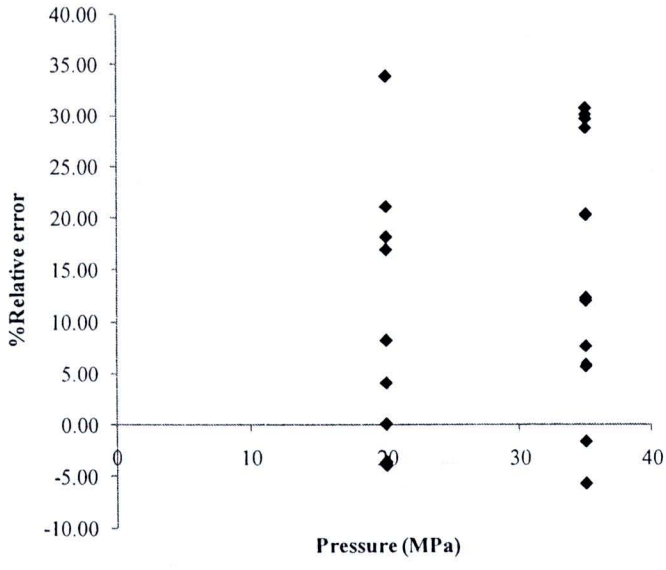

Figure 6.8 The relationship between percentage of relative error of calculated value from Eq. 6.6 and pressure.

Within the temperature range of 320 – 350 °C, the calculated %ME values were higher than experimented values because the observed %ME was presumed to be reduced by the thermal degradation reaction. Indeed, RBD palm olein oil consists of approximately 46% oleic acid and 11% linoleic acid, respectively [97]. It has been reported that thermal degradation of unsaturated fatty acids occurs at the same temperature range and residence time of 320 – 350 °C over 30 min For example, methyl oleate and methyl linoleate decompose by approximately 10% and 20% by weight, respectively, in SCM at 350 °C after 30 min contact time [58]. Therefore, by extrapolation to this system, 4.6% and 2.2% of methyl oleate and linoleate, respectively, were degradable and so the observed ME content was reduced by 6.8% at 350 °C for over 30 min residence time.

Variation in the compressibility factor slows down the rate of transesterification slightly, as shown by comparison with calculated values from equation (6.6), which accounts only for chemical kinetics, and which were approximately 2 – 13% higher than the values derived from equation (6.7). At a temperature of 280 °C, the difference between the calculated values derived from equations (6.6) and (6.7) decreased with increasing methanol to oil molar ratios due to the irreversible assumption of kinetic model was more valid at high methanol to oil molar ratio [72]. This can be observed, for instance, by comparison of the difference between the calculated values in either runs 1 and 3 or runs 2 and 4. However, the effect of the changes in the compressibility factor upon the rate of transesterification had the same magnitude, being approximately 10%, at temperatures above 300 °C.

An example of the change in the compressibility factor and the molar volume of the mixture are shown in Figures 6.9 and 6.10, respectively. Values from run nos. 1 – 5 were selected to demonstrate the effect of pressure on the changes in the compressibility factor, which, as expected, were higher at 35.0 MPa than at 20.0 MPa. In addition, the values from run nos. 17 and 22 illustrate the effect of temperature on the changes in the compressibility factor and the molar volume of mixture. It was clear that the compressibility factor and molar volume at ~350 °C rose faster than the values at ~280 °C. At a constant temperature and pressure, the changes in the compressibility factor and the molar volume at a low methanol to oil molar ratio was faster than that seen at a high methanol to oil molar ratio. Therefore, the compressibility factor and the molar volume of the mixture were both enhanced with increasing reactor length and they had a steeper slope at high temperatures and lower methanol to oil molar ratios.

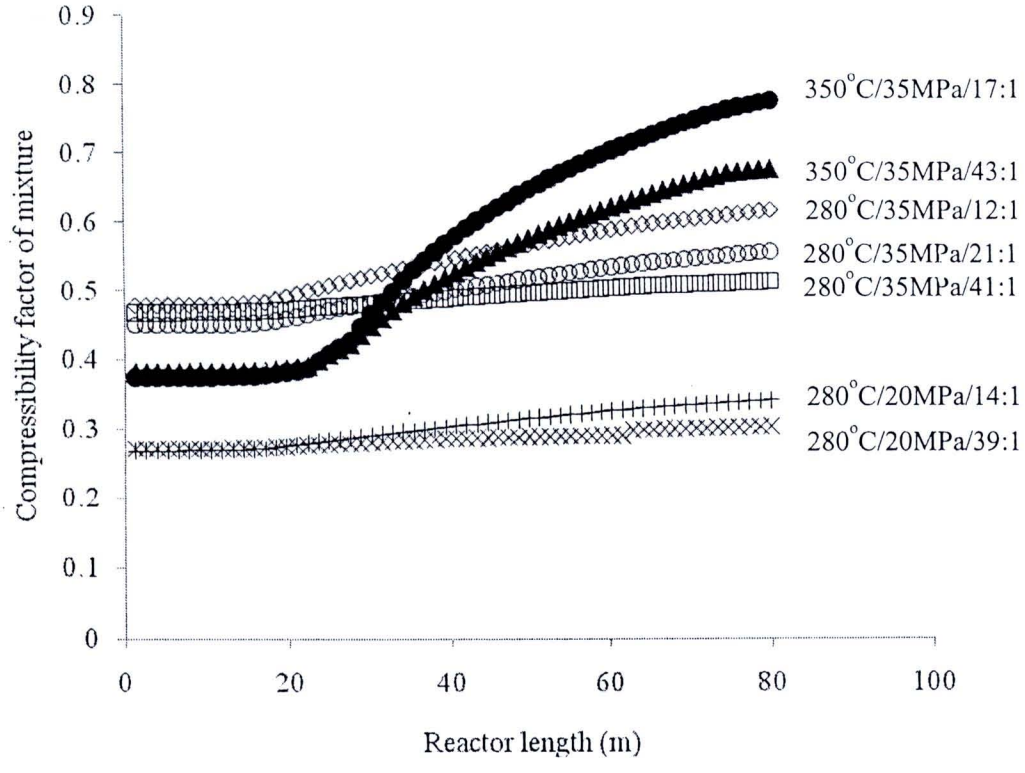

Figure 6.9 The changes in the compressibility of the reaction mixture along the length of the tubular reactor in run no. 1 (◇), 2 (+), 3 (□), 4 (×), 5 (○), 17 (●) and 22 (▲). The abbreviations on the figure are the experimental conditions as the operational temperature (°C)/pressure (MPa)/methanol to oil (molar ratio).

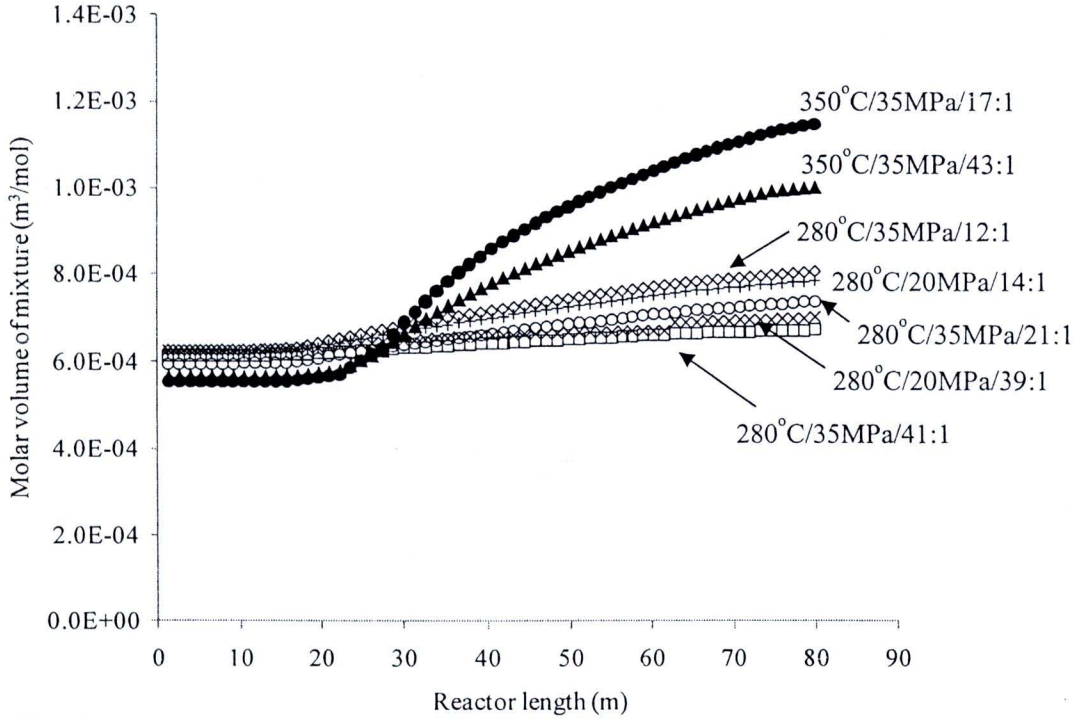

Figure 6.10 The changes in the molar volume of the reaction mixture along the length of the tubular reactor in run no. 1 (◇), 2 (+), 3 (□), 4 (×), 5 (○), 17 (●) and 22 (▲). The abbreviations on the figure are the experimental conditions as the operational temperature (°C)/pressure (MPa)/methanol to oil (molar ratio).

The deviation of the predicted %ME values at high temperatures may be due to a number of reasons. Firstly, the real mixture is slightly different from the simulated mixture, as mentioned in Section 3.1. Since the exact chemical formula of vegetable oils does not exist, the deviation from this cause could not be avoided but could probably be minimized by some approaches, such as using a group contribution method to estimate a single pseudo-triglyceride molecule [56, 57, 86]. Secondly, thermodynamic model predictions at high temperatures have, in general, a higher relative error than at low temperatures. For example, the PR-MHV2-UNIQUAC prediction of glycerol + methanol system had maximum relative error of 10% at 523 K compared to 5% at 493 K. Thirdly, the coefficient of determination of kinetics model at 0.9578 [72], ~4% of random error was taken into account in our compressible flow model.

6.4. Residence time estimation procedure

Refer to Equation 6.9, this is the general residence time estimation in tubular reactor [98].

$$\tau = \int_{V} \frac{dV}{u} \tag{6.9}$$

where V and u are reactor volume (m^3) and linear velocity of fluid (m/sec), respectively. Since, the differential reactor volume can be decomposed to the product of cross-sectional area and reactor length, while the linear velocity is the product of total molar flow rate and molar volume of the mixture, then Equation 6.9 can be rewritten as Equation 6.10.

$$\tau = \frac{A}{F_0 / A} \int_{L} \frac{dL}{v(L)} \tag{6.10}$$

The development of molar volume of mixture can be separated into constant and increasing interval as illustrate in Figure 6.10, Equation 6.10 is rewritten as Equation 6.11 then simplify to Equation 6.12.

$$\tau = \frac{A^2}{F_0}\left[\int_{0}^{L_1} \frac{dL}{v_m(L)} + \int_{L_1}^{80} \frac{dL}{v_m(L)}\right] \tag{6.11}$$

$$\tau = \frac{A^2}{F_0}\left[\frac{L_1}{v_1} + \int_{L_1}^{80} \frac{dL}{v_m(L)}\right] \tag{6.12}$$

where A, F, v, and L are reactor cross-sectional area (m^2), total molar flow rate (mol/s), molar volume (m^3/mol) and reactor length (m), respectively. The subscript 0, 1 and m refer to reactor inlet, constant molar volume interval and mixture, respectively. The development of molar volume within increasing interval as a function of reactor length, v_m (L), can be evaluated by fitting of cubic polynomial to PR-MHV2-UNIQUAC model prediction and integrated numerically by adaptive Gauss-Kronrod method in Matlab® software.